Synthesis and Structural Transformation of Zirconia Aerogels

David A. Ward and Edmond I. Ko*

Department of Chemical Engineering, Carnegie Mellon University
Pittsburgh, Pennsylvania 15213

Received January 19, 1993. Revised Manuscript Received April 15, 1993

Zirconia (ZrO_2) aerogels were prepared by the sol-gel method using zirconium *n*-propoxide in *n*-propanol followed by supercritical drying with carbon dioxide. This synthesis, without the use of dopants, formed a high surface area material and stabilized the tetragonal phase at low temperatures. By optimizing the water and nitric acid amounts, we formed a zirconia aerogel with a surface area of ca. 130 m^2/g after calcination 773 K for 2 h. The effect of heat treatment on the physical characteristics of the aerogel was determined by nitrogen adsorption, X-ray diffraction, Raman spectroscopy, electron microscopy, and differential thermal analysis. The untreated, highly porous, amorphous aerogel decreased in surface area and pore volume upon heating. By variation of the heat treatment, the zirconia aerogel existed in either a completely amorphous, tetragonal, or monoclinic form at room temperature. In situ X-ray diffraction measurements were used to examine the tetragonal-to-monoclinic phase transformation, which was controlled by embryo formation and growth and was not a simple function of crystallite size. Finally, the time required for gel formation controlled the type of oxide network formed, which in turn dictated the physical characteristics of the aerogel and the number of defects for embryo formation.

Introduction

Aerogels are high-surface-area, high-porosity materials prepared by the sol-gel method followed by supercritical extraction. In 1931, Kistler was the first to prepare aerogels[1,2] and to recognize their potential application as catalysts because of their high surface area per mass.[3] More recently, Teichner *et al.*[4] prepared many different aerogels (SiO_2, Al_2O_3, TiO_2, ZrO_2, MgO, and mixed oxides) as potential catalysts. In addition to their varied catalytic uses,[5] aerogels have applications in many other areas, such as insulation, ceramics, and Cerenkov detectors.[6,7]

The first step in the preparation of aerogels is to form an alcogel by the sol-gel method. The sol-gel method[8,9] consists of two steps: hydrolysis and condensation. With a metal alkoxide ($M(OR)_n$) as precursor, the hydrolysis step can be written as

$$M(OR)_n + xH_2O \rightarrow M(OR)_{n-x}(OH)_x + xROH \quad (1)$$

This reaction is usually carried out in a nonaqueous solvent and is catalyzed by either an acid or a base. The partially hydrolyzed intermediate then undergoes a condensation reaction:

$$M\text{-}OH + M\text{-}OX \rightarrow M\text{-}O\text{-}M + XOH \quad (2)$$

forming an M-O-M bridge by the removal of either water (X = H) or alcohol (X = R). The final product of the sol-gel reactions, a network consisting of M-O-M bridges, depends greatly on the choice of conditions,[9] often called the sol-gel parameters. Two of the important sol-gel parameters are the hydrolysis ratio, defined as the number of moles of water per mole of precursor used, and the amount and type of catalyst used.[9] Other parameters include the choice of precursor and solvent,[9] the precursor concentration,[10] and the temperature of reaction.[10]

After formation of the alcogel, the liquid solvent is removed by supercritical extraction to prepare an aerogel.[11] During conventional drying, a liquid-vapor interface forms in the pores of the material. The surface tension at this interface collapses the weak pores. However, supercritical extraction eliminates this problem by replacing the liquid solvent with a supercritical fluid that cannot form a liquid-vapor interface. The supercritical fluid can then be removed from the porous gel network without causing damage. This technique has evolved[11] from using alcohol as the supercritical medium in a batch process[1] to using the safer supercritical CO_2 in a semicontinuous fashion.[12]

Aerogels have many unique and interesting properties that enhance their use as catalysts. In our laboratory, we have prepared a niobia (Nb_2O_5) aerogel that has a surface area nearly four times as large as a precipitated sample.[13] In addition, this aerogel is X-ray amorphous while the precipitated niobia is crystalline after calcination at 773 K for 2 h. This is catalytically important because the amorphous phase has been shown to have a higher acidity than the crystalline phase.[14] We have also studied the

* To whom correspondence should be addressed.

(1) Kistler, S. S. *Nature* **1931**, *127*, 741.
(2) Kistler, S. S. *J. Phys. Chem.* **1932**, *36*, 52.
(3) Kistler, S. S.; Swann, Jr., S.; Appel, E. G. *Ind. Eng. Chem.* **1934**, *26*, 388.
(4) Teichner, S. J.; Nicolaon, G. A.; Vicarini, M. A.; Gardes, G. E. E. *Adv. Colloid Interface Sci.* **1976**, *5*, 245.
(5) Pajonk, G. M. *Appl. Catal.* **1991**, *72*, 217.
(6) Gesser, H. D.; Goswami, P. C. *Chem. Rev.* **1989**, *89*, 765.
(7) Teichner, S. J. *Rev. Phys. Appl.* **1989**, *24*, C4-1.
(8) Brinker, C. J.; Scherer, G. W. *Sol-Gel Science: The Physics and Chemistry of Sol-Gel Processing*; Academic: Boston, 1990.
(9) Livage, J.; Henry, M.; Sanchez, C. *Prog. Solid State Chem.* **1988**, *18*, 259.
(10) Yoldas, B. E. *J. Polym. Sci.* **1986**, *24*, 3475.
(11) Ayen, R. J.; Iacobucci, P. A. *Rev. Chem. Eng.* **1988**, *5*, 157.
(12) Cheng, C.-P.; Iacobucci, P. A.; Walsh, E. N. U.S. Patent 4,619,908; Oct 28, 1986.
(13) Ko, E. I.; Maurer, S. M. *J. Chem. Soc., Chem. Commun.* **1990**, *15*, 1062.
(14) Maurer, S. M.; Ko, E. I. *J. Catal.* **1992**, *135*, 125.

0897-4756/93/2805-0956$04.00/0

Table I. Literature Values of Zirconia Surface Area

preparation method	heat treatment	surface area (m^2/g)	pore vol (cm^3/g)	ref
zirconium isopropylate hydrolyzed in isopropanol followed by supercritical evaporation of solvent	673 K in air for 8 h	81	0.17	4
zirconyl chloride precipitation with ammonia and water at pH = 10	723 K in air for 15 h	111	0.112	30
zirconyl nitrate precipitation with gaseous ammonia and water	770 K in air for 2 h	126	0.13	31
zirconium *n*-propoxide mixed with acetic acid and *n*-propanol followed by supercritical evaporation of solvent	none	410–480[a]	8.7–0.6[a]	34

[a] Dependent on precursor concentration.

preparation of titania (TiO_2) aerogels.[15] Again, our titania aerogel was found to have about 4 times the surface area of a commercially available titania catalyst after the same heat treatment, and we synthesized a pure anatase sample, while the commercially available material is a mix of anatase and rutile. So, we have seen that aerogel preparation can both yield a higher surface area material and stabilize particular structures. Both of these features are beneficial for catalyst function.

We applied aerogel technology to zirconium oxide (zirconia, ZrO_2) in order to make a high surface area catalyst and catalyst support. Zirconia has several properties important for catalytic applications. Its surface has both acidic and basic properties, as well as both oxidizing and reducing properties.[16] It has been shown to be an excellent support for (a) CuO for methanol synthesis from CO_2 and H_2,[17] (b) La–Cu oxide for the reduction of NO by CO,[18] and (c) Rh for the hydrogenation of CO and CO_2 to hydrocarbons.[19] In addition, sulfate promoted zirconia is a superacid[20] and active in many different reactions.[21] As a catalyst, zirconia is active in the isosynthesis reaction of CO/H_2[22] and the isomerization and hydrogenation of 1-butene.[23]

Zirconia preparation by the sol–gel method has been extensive. This is because zirconia is a good refractory material, and the sol–gel method is widely used as a route for making ceramics. Yoldas[24,25] formed zirconium oxide by the hydrolytic condensation of zirconium alkoxides. He found that the product zirconia was dependent on sol–gel parameters such as water/alkoxide ratio,[24] choice and amount of alkoxide used, and choice and amount of acid used.[25] In a different synthesis, a gel was prepared by reacting water and zirconium *n*-propoxide in the solvent 2-propanol in the presence of acetic acid.[26] Another similar synthesis used nitric acid, instead.[27] A fourth method mixed the *n*-propoxide in cyclohexane and allowed hydrolysis to occur with moisture in air.[28] In addition to the use of alkoxides as a precursor, zirconium salts can be used to form precipitates from the sol–gel method. These precursor salts include $ZrOCl_2$,[29,30] $ZrO(NO_3)_2$,[31] $ZrO(CH_3COO)_2$,[32] $ZrCl_4$, and $Zr(NO_3)_4$.[33]

The literature on the preparation of zirconia aerogels is very limited. Teichner *et al.*[4] formed an aerogel by hydrolyzing zirconium isopropylate (isopropoxide) in both benzene and isopropyl alcohol and then supercritically evacuating the solvent. Vesteghem *et al.*[34] gelled a zirconium *n*-propoxide, acetic acid, and 1-propanol mixture without the addition of water. Again, supercritical evacuation of the propanol yielded a zirconia aerogel.

The goal of most of the above work was to form a dense ceramic and no attempt was made to prepare a high surface area zirconia. Table I shows a representative list of surface areas and heat treatments that have been reported in the literature. Treatment to temperatures above ca. 773 K caused the surface area to decrease even further.[16,30,31] A zirconia aerogel might have both a higher surface area and a high resistance to sintering during heat treatment.

In this work, we synthesized a high surface area, porous zirconium oxide aerogel for use as a catalyst and catalyst support. In doing so, we examined the effects of changing the sol–gel parameters on the structure and characteristics of the aerogel. We also performed a comprehensive study of the effects of heat treatment on this aerogel. From these results, we showed that a specific zirconia structure can be "tuned" by the choice of preparation parameters and heat treatment conditions.

Experimental Section

Zirconia aerogels were formed by first making an alcogel. The zirconium precursor used was zirconium *n*-propoxide (Alfa Chemicals, 70% in propanol). We used a zirconium concentration of 1.0 mmol of Zr^{4+}/mL of *n*-PrOH (including the propanol in the precursor). The amount of hydrolysis water used was varied from 2.0 mol of H_2O/mol of Zr^{4+} to 7.0 mol/mol. Finally, nitric acid (Fisher, 70% w/w) was added as a catalyst.

In one beaker, the appropriate amount of distilled water was added to 15 mL of *n*-propanol (Fisher, Certified). A second solution was prepared by mixing the desired amount of HNO_3, 15 mL of alcohol, and in a nitrogen purged glovebox, 16.2 mL of the precursor. The water/alcohol solution was quickly added to the precursor/acid/alcohol solution after its removal from the glovebox. The mixture was vigorously stirred by a magnetic stir bar until a gel formed. The gel time was defined as the time required after mixing for the vortex created by the stirring to disappear completely.

The gel was covered and allowed to age for 2 h at room temperature. The alcohol was then removed by supercritical

(15) Campbell, L. K.; Na, B. K.; Ko, E. I. *Chem. Mater.* **1992**, *4*, 1329.
(16) Tanabe, K. *Mater. Chem. Phys.* **1985**, *13*, 347.
(17) Amenomiya, Y. *Appl. Catal.* **1987**, *30*, 57.
(18) Mizuno, N.; Yamato, M.; Tanaka, M.; Misono, M. *J. Catal.* **1991**, *132*, 560.
(19) Iizuka, T.; Tanaka, Y.; Tanabe, K. *J. Catal.* **1982**, *76*, 1.
(20) Hino, M.; Arata, K. *J. Chem. Soc., Chem. Commun.* **1980**, 851.
(21) Tanabe, K.; Yamaguchi, T. In *Successful Design of Catalysts*; Inui, T., Ed.; Elsevier: Amsterdam, 1988; pp 99–110.
(22) Tseng, S. C.; Jackson, N. B.; Ekerdt, J. G. *J. Catal.* **1988**, *109*, 284.
(23) Pajonk, G. M.; El Tanany, A. *React. Kinet. Catal. Lett.* **1992**, *47*, 167.
(24) Yoldas, B. E. *J. Am. Ceram. Soc.* **1982**, *65*, 387.
(25) Yoldas, B. E. *J. Mater. Sci.* **1986**, *21*, 1080.
(26) Wolf, C.; Rüssel, C. *J. Mater. Sci.* **1992**, *27*, 3749.
(27) Ayral, A.; Assih, T.; Abenoza, M.; Phalippou, J.; Lecomte, A.; Dauger, A. *J. Mater. Sci.* **1990**, *25*, 1268.
(28) Kundu, D.; Ganguli, D. *J. Mater. Sci. Lett.* **1986**, *5*, 293.
(29) Benedetti, A.; Fagherazzi, G.; Pinna, F. *J. Am. Ceram. Soc.* **1989**, *72*, 467.
(30) Mercera, P. D. L.; Van Ommen, J. G.; Doesburg, E. B. M.; Burggraaf, A. J.; Ross, J. R. H. *Appl. Catal.* **1990**, *57*, 127.
(31) Duchet, J. C.; Tilliette, M. J.; Cornet, D. *Catal. Today* **1991**, *10*, 507.
(32) Jada, S. S.; Peletis, N. G. *J. Mater. Sci. Lett.* **1989**, *8*, 243.
(33) Srinivasan, R.; Harris, M. B.; Simpson, S. F.; DeAngelis, R. J.; Davis, B. H. *J. Mater. Res.* **1988**, *3*, 787.
(34) Vesteghem, H.; Jaccon, T.; Lecomte, A. *Rev. Phys. Appl.* **1989**, *24*, C4-59.

drying with carbon dioxide.[12] In a supercritical extraction screening system (Autoclave Engineers, Model 08U-06-60FS), supercritical CO_2 was flowed through the gel at ca. 343 K and 20.7×10^3–24.7×10^3 kPa with a downstream flow rate of 85 L/h at atmospheric pressure and room temperature. The alcohol was completely replaced by CO_2 after approximately 2 h. After removal of the CO_2, the resultant powder, an aerogel, was ground into a powder of <100 mesh.

The first heat treatment step was to dry the powder at 383 K for 3 h under a vacuum of 3.4 kPa. Subsequent calcinations were performed under flowing oxygen (24 L/h) in a quartz tube inside a tubular furnace. The sample was heated at a rate of 10 K/min to the desired temperature and held at that temperature for 2 h. The dried powder was calcined to 673 and 773 K. Further calcinations to 973 and 1173 K were performed on a sample previously heated to 773 K.

An Autosorb-1 gas sorption system (Quantachrome Corp.) was used to obtain nitrogen adsorption/desorption isotherms. Before analysis, all samples were outgassed for 3 h under vacuum at either room temperature (non-heat-treated samples), 373 K (vacuum-dried samples), or 473 K (all calcined samples). From the 40-point adsorption and desorption isotherms, BET surface area (taken at $P/P_0 \sim 0.3$), total pore volume (P/P_0 close to unity), and pore size distribution (BJH method)[35] were calculated.

Crystal structure determinations were made by X-ray diffraction (XRD), Raman spectroscopy, and high-resolution electron microscopy (HRTEM). X-ray diffraction experiments were performed on a Rigaku D/Max Diffractometer with Cu Kα radiation. When required, the X-ray diffraction patterns were fit using commercial peak fitting software (Jandel Scientific Peak Fit). Peaks were fit as Voigt functions with a constant background. The volume fractions of the tetragonal and monoclinic phases of zirconia were determined following the method of Toraya *et al.*[36] First, integrated peak intensities of the tetragonal (111) peak and the ($\bar{1}11$) and (111) monoclinic peaks were determined. [Note: In the literature, the labeling of the tetragonal peak will vary between (111) for a face centered lattice and (101) for a body centered lattice.] An intensity ratio was then defined as

$$X_m = \frac{I_m(\bar{1}11) + I_m(111)}{I_m(\bar{1}11) + I_m(111) + I_t(111)} \quad (3)$$

Finally, the volume fraction of the monoclinic phase was determined from

$$v_m = \frac{1.311X_m}{1 + 0.311X_m} \quad (4)$$

Raman spectra were obtained with the 514.5-nm line of a Spectra Physics Model 2505-5-W argon ion laser.[37] HRTEM was performed on a JEOL 4000EX. Microscopy samples were prepared by placing two drops of an aerogel/2-propanol dispersion on a holey carbon grid. The 2-propanol was allowed to evaporate leaving the aerogel deposited on the grid. A Perkin-Elmer DTA 1700 high-temperature thermal analyzer with thermal analysis data station was used for differential thermal analysis scans with a heating rate of 10 K/min.

Selected samples were examined at elevated temperatures by in situ X-ray diffraction using a Rigaku high-temperature X-ray diffraction attachment for θ–θ goniometer. Platinum wires circling the sample stage allowed for controlled heating to temperatures up to 1573 K. Samples were heated in static air at a rate of 10 K/min to the desired temperature and held at that temperature for a specific amount of time. Cooling occurred at 100 K intervals with the temperature allowed to equilibrate after each step. Diffraction patterns were taken at various times during heating, holding, and cooling. Crystallite size was determined by X-ray line broadening using Scherrer's equation.[38] The full width at half-maximum and peak center were determined with the fit data described above.

(35) Barrett, E. P.; Joyner, L. G.; Halenda, P. P. *J. Am. Chem. Soc.* **1951**, *73*, 373.
(36) Toraya, H.; Yoshimura, M.; Sōmiya, S. *J. Am. Ceram. Soc.* **1984**, *67*, C-119.
(37) Serghiou, G. C.; Hammack, W. S. *J. Chem. Phys.* **1992**, *96*, 6911.
(38) Klug, H. P.; Alexander, L. E. *X-ray Diffraction Procedures*; Wiley: New York, 1974.

Table II. Summary of Gel and Aerogel Data

gel no.	H_2O/Zr^{4+} (mol/mol)	HNO_3 (mL)	HNO_3/Zr^{4+} (mol/mol)	gel time (s)	surface area[a] (m^2/g)	pore vol[a] (cm^3/g)
			Series A			
35	4.0	1.75	0.761	0-prec	n/a[b]	n/a
46	4.0	1.90	0.826	0-gel	84	n/a
43	4.0	2.05	0.891	7	111	n/a
42	4.0	2.20	0.956	10	102	n/a
45	4.0	2.35	1.021	18	92	n/a
39	4.0	2.40	1.043	4680	n/a	n/a
36	4.0	2.50	1.087	30000	93	n/a
			Series B			
65	2.0	1.75	0.761	12	94	n/a
64[c]	2.0	1.90	0.826	14	124	n/a
60	2.0	2.05	0.891	50	99	n/a
62	2.0	2.20	0.956	800	81	n/a
			Series C			
A6	2.0	0.00	0.000	0-prec	12	0.1041
A5	2.0	1.60	0.695	8	130	0.3954
B0	2.0	1.75	0.761	20	134	0.3722
73[c]	2.0	1.90	0.826	35	112	0.3232
A0	2.0	2.17	0.943	266	69	0.2791
			In Situ Samples			
75[c]	2.0	1.90	0.826	34	n/a	n/a
82[c]	2.0	1.90	0.826	21	119	n/a

[a] Surface area and pore volume of samples determined after calcination at 773 K for 2 h. [b] n/a = not available. [c] Our synthesis contained batch-to-batch variation, accounting for different gel times among series at the same water and acid amounts. This variation did not affect the qualitative conclusion on the physical characteristics of these gels (see text).

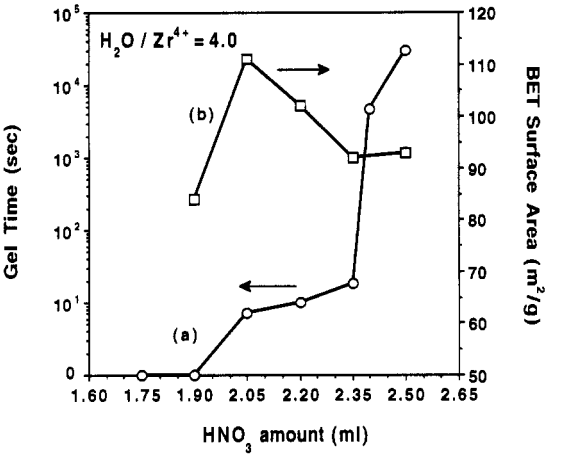

Figure 1. Effect of acid amount on (a) gel time and (b) surface area after calcination at 773 K for 2 h. These data were obtained at an H_2O/Zr^{4+} ratio of 4.0 (gel series A).

Results

Effect of Sol–Gel Parameters. To determine the effect of sol–gel parameters on the formation and properties of zirconia aerogels, we prepared a series of alcogels made with different acid and water contents. We first examined the effect of acid ratio on the gel time and surface area of the aerogel. At a constant water to zirconium molar ratio of 4.0, we made gels using different amounts of nitric acid (see Table II, series A). The change in gel time with acid amount is shown in Figure 1, curve a. Before the addition of the water solution, the precursor solution was clear and gold. When 1.75 mL of acid or less was used, a white precipitate formed immediately upon addition of the water. When a greater amount of acid was used,

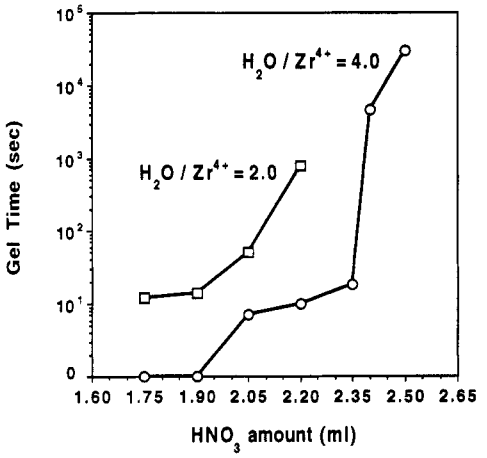

Figure 2. Relationship between gel time and acid amount for H_2O/Zr^{4+} ratios of 2.0 (gel series B, □) and 4.0 (gel series A, ○).

precipitation was prevented to varying degrees; instead, a solid gel was formed. With 1.90 mL of acid, a gel was formed immediately. The gel was opaque white, indicating some precipitates were trapped in the gel. The use of 2.05 mL and 2.20 mL of acid yielded gel times of 7 and 10 s, respectively. Both of these gels were milky white. Using 2.35 mL increased the gel time to 18 s, and the gel was golden and only slightly cloudy. A larger acid amount at this point drastically increased the gel time. An increase in acid of only 0.05 mL (to 2.40 mL) lengthened the gel time to 78 min. The gel was completely clear and golden. Finally, a solution with 2.5 mL of acid required a full day to gel.

The above series of gels were extracted and heat treated to 773 K, a common catalyst pretreatment temperature. Their BET surface areas are shown in Figure 1, curve b. The maximum surface area of 111 m^2/g occurred at an acid amount of 2.05 mL. More or less acid decreased the surface area.

We examined the effect of water ratio by performing a similar set of experiments with $H_2O/Zr^{4+} = 2.0$ (Table II, series B). At each acid amount, decreasing the water content increased the gel time (see Figure 2). In particular, at an acid amount of 2.05 mL, the gel with a water ratio of 2.0 had a slightly cloudy gold color and required 50 s to form. Increasing the water ratio to 4.0 dropped the gel time to 7 s, and the gel was much more cloudy. At this acid amount, gels with a water ratio up to 7.0 were made. The gel time continued to decrease with increasing water ratio until the gel time was 0 s at 7.0, at which point the gel was opaque. At each water ratio, the gel time behavior with respect to acid content was identical, with larger acid contents increasing the gel time. The surface area results for both water ratios are shown in Figure 3. The general shape of the curves is the same. The larger water ratio shifted the curve to higher acid amounts.

Effect of Heat Treatment. To study the effect of heat treatment on the aerogel, we made a gel with a water ratio of 2.0 and acid content of 1.90 mL (Gel No. 73 from series C of Table II). Not only did this formulation form a hard gel that was easily extracted, but it also exhibited the highest surface area in the initial screening. Nitrogen adsorption/desorption isotherms taken after each heat treatment step were used to show the effect of heat treatment on the pore structure of the aerogel. Figure 4 shows the results for surface area and pore volume. Immediately after extraction, the zirconia aerogel had a surface area of over 300 m^2/g and a pore volume of 0.91

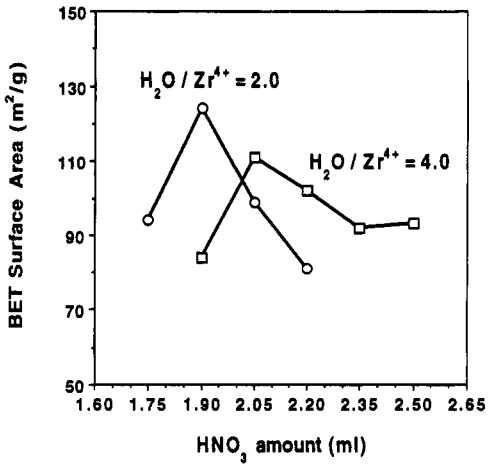

Figure 3. BET surface areas of ZrO_2, after calcination at 773 K for 2 h, as a function of acid and water content (gel series A and B).

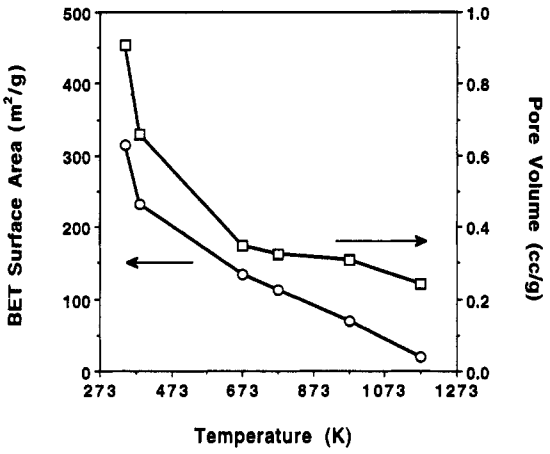

Figure 4. Effect of heat treatment, calcination for 2 h at the given temperature, on the surface area and pore volume of ZrO_2 aerogels (gel no. 73).

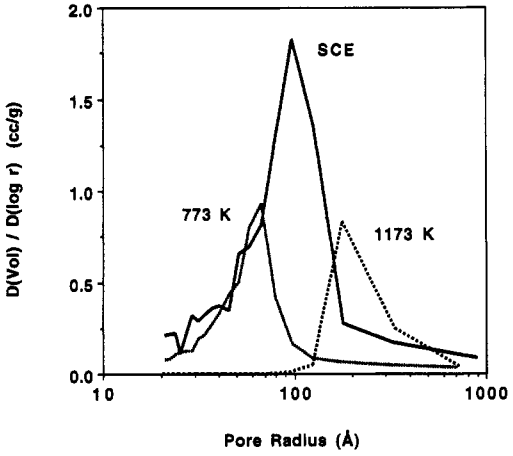

Figure 5. Effect of heat treatment on the pore size distribution of ZrO_2 aerogels (gel no. 73). The data were analyzed with a 40-point nitrogen desorption isotherm. SCE refers to the as extracted sample. Actual data points are not shown in the figure for clarity.

cm^3/g. With calcination at 773 K for 2 h, these values decreased to 112 m^2/g and 0.32 cm^3/g. Further treatment to 1173 K dropped the surface area to 20 m^2/g while the pore volume remained relatively constant at 0.24 cm^3/g. The pore size distribution of this aerogel also changed with heat treatment, as seen in Figure 5. The sample was primarily mesoporous with a pore size distribution centered

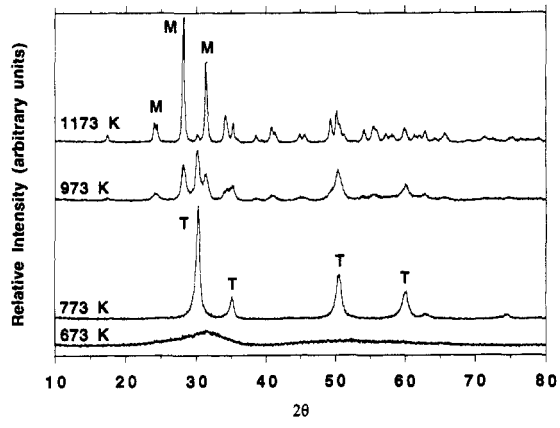

Figure 6. X-ray diffraction patterns of ZrO_2 aerogels (gel no. 73) after calcination at the indicated temperature for 2 h.

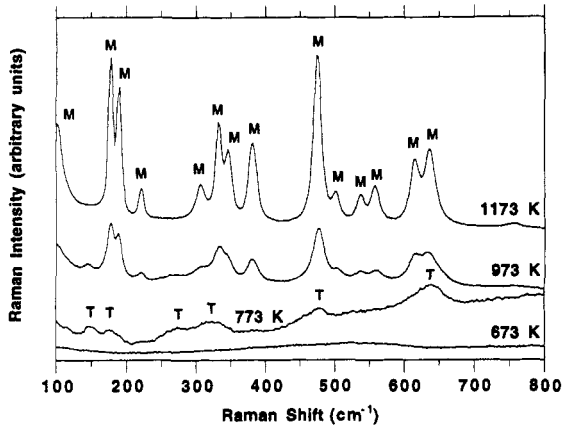

Figure 7. Raman spectra of ZrO_2 aerogels (gel no. 73) after calcination at the indicated temperature for 2 h.

around 100 Å after extraction. Heat treatment caused the distribution to change, with a distribution centered around 65 Å and 200 Å for calcination at 773 K and 1173 K, respectively.

X-ray diffraction and Raman spectroscopy were used for crystal structure determinations. As shown in Figures 6 and 7, the zirconia aerogel (gel no. 73) was both X-ray and Raman amorphous after heat treatments of 673 K and below. After a heat treatment of 773 K, crystallization occurred. The X-ray diffraction pattern can be indexed as either the cubic or tetragonal phase, as these two phases are very hard to distinguish by normal X-ray diffraction techniques.[33] However, Raman spectroscopy easily distinguishes between the two.[33] Cubic zirconia has a single Raman peak at 490 cm^{-1} whereas the tetragonal phase has multiple Raman bands, with the strongest being at 148, 179, 263, 473, and 640 cm^{-1}.[39] The Raman spectrum at 773 K clearly showed the multiple tetragonal bands. The amorphous zirconia aerogel thus crystallized into the tetragonal phase after treatment at 773 K. Both Raman and X-ray diffraction data showed that heating to higher temperatures caused the zirconia to transform into the monoclinic phase (14 observed Raman bands). This transformation was almost complete by 1173 K.

To gain further insight into the structure of the amorphous material and how it crystallized, we used high-resolution electron microscopy to examine more closely the zirconia structure. In the microscope, we looked at a sample (gel no. 73) that had been heated at 673 K for 2 h. This sample was both X-ray and Raman amorphous. The HRTEM diffraction pattern and bright field image of this sample are shown in Figure 8. Under the microscope, this material was observed to be not truly amorphous but to contain small crystallites. The diffraction pattern consisted of multiple rings. These rings can be indexed to the tetragonal phase, and their presence showed that the material was polycrystalline. The bright field image showed crystallites with sizes under 100 Å. In an effort to find an amorphous zirconia aerogel at the atomic level, we also examined by HRTEM a sample which had only been heat treated at 623 K. While this sample appeared amorphous upon initial examination under the microscope, small crystallites of the tetragonal phase formed quickly due to heating from the electron beam. The important observation was that our initially amorphous zirconia aerogel always crystallized into the tetragonal phase first.

Differential thermal analysis was performed on a vacuum-dried aerogel (gel no. 73) to learn more about the crystallization of zirconia. The DTA scan (see Figure 9) showed two exothermic peaks, one around 473 K and the second just below 773 K. The first peak was associated with the decomposition of surface residuals and the second with the crystallization of the tetragonal phase.

For comparison, the effect of heat treatment on ZrO_2 obtained from Degussa (VP zirconium oxide) was determined. This zirconia was formed by the high-temperature hydrolysis of $ZrCl_4$. A comparison of surface area, pore volume, and structure between our zirconia aerogel and Degussa zirconia is shown in Figure 10. Degussa zirconia had a surface area of 44 m^2/g with heating at or below 973 K. This surface area was lower than that for our aerogel (Figure 10a), but the difference became less at higher temperatures. In Figure 10b we see that the Degussa zirconia had a higher pore volume (0.7 cm^3/g) after moderate heat treatments. The pore size distribution (Figure 10c) showed that the Degussa sample consisted primarily of macropores, accounting for its high pore volume but low surface area. Finally, Figure 10d shows that, in the temperature range studied, the zirconia aerogel can be made in a single phase (either amorphous, tetragonal or monoclinic) while the Degussa zirconia was always a mixture of the tetragonal and monoclinic phases.

Observation of the Tetragonal-to-Monoclinic (T → M) Transformation. At atmospheric pressure, zirconia can exist in three structures: monoclinic, tetragonal, and cubic. In the bulk, the monoclinic phase is stable below 1443 K. The tetragonal phase has been observed at temperatures between 1443 and 2643 K. Finally, the cubic phase is stable from 2643 K up to the melting point of zirconia at 2953 K. The transformation between the monoclinic and tetragonal phases is martensitic.[40,41]

The phase diagram for zirconia seems to be in contrast with our structural results from above. Our zirconia aerogel crystallized into the tetragonal phase at low temperatures, instead of the stable bulk monoclinic phase. Only upon heating to higher temperatures did the monoclinic phase form. To better understand the structural evolution of the aerogel, we examined the structure of the material in situ during heating and cooling.

In situ X-ray diffraction experiments were performed on a zirconia aerogel (gel no. 75) that had been previously

(39) Phillippi, C. M.; Mazdiyasni, K. S. *J. Am. Ceram. Soc.* 1971, *54*, 254.

(40) Subbarao, E. C. In *Advances in Ceramics, Science and Advances in Zirconia*; Heuer, A. H., Hobbs, L. W., Eds.; American Ceramics Society: Columbus, OH, 1981; Vol 3, pp 1–24.

(41) Subbarao, E. C.; Maiti, H. S.; Srivastava, K. K. *Phys. Status Solidi A* 1974, *21*, 9.

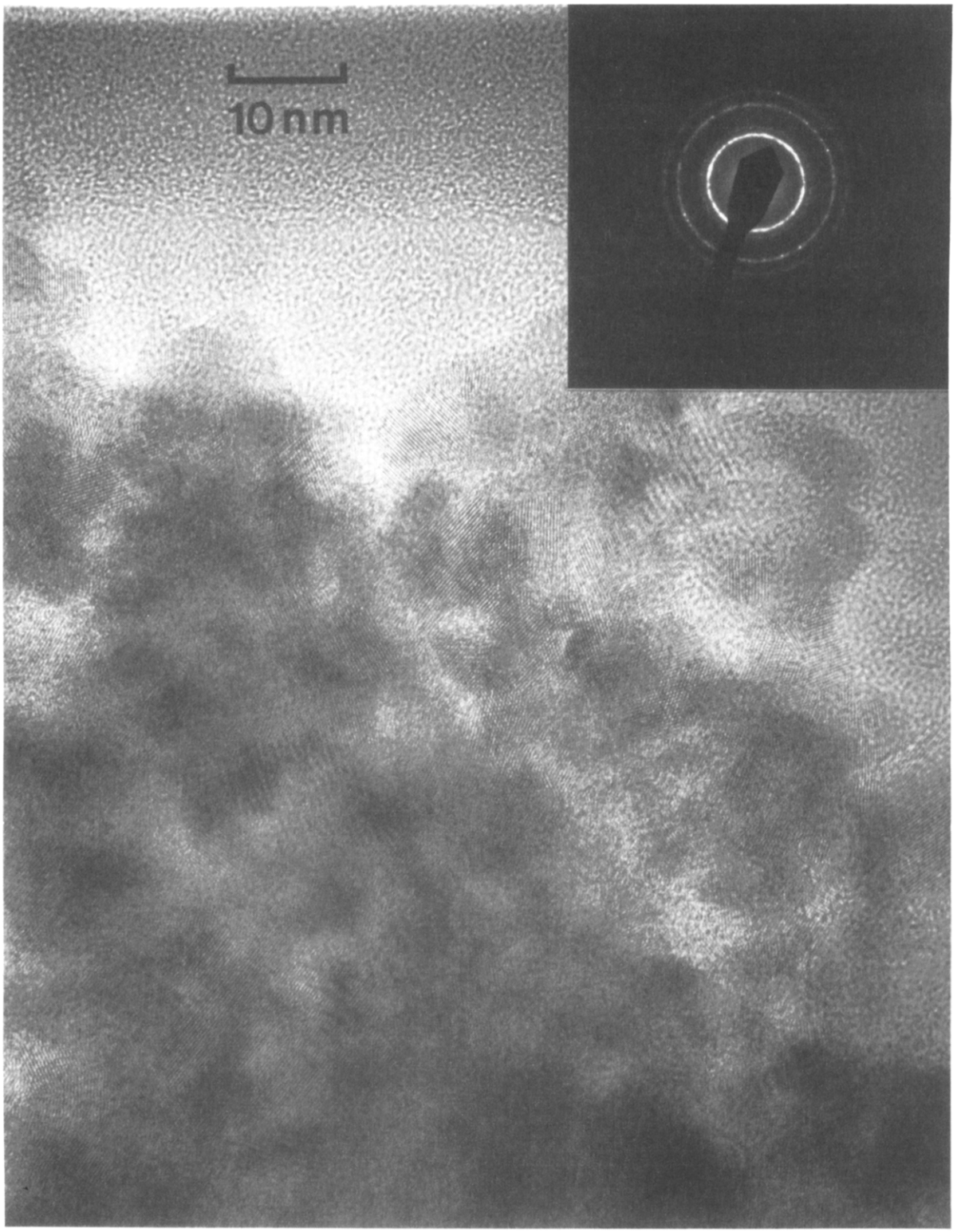

Figure 8. High resolution transmission electron micrograph of an X-ray amorphous ZrO_2 aerogel (gel no. 73) that had been calcined at 673 K for 2 h. The inset is a diffraction pattern indexed to be the tetragonal phase.

heated at 773 K for 2 h in oxygen and was in the tetragonal phase. In three separate experiments, this tetragonal sample was heated in situ to a maximum temperature of 973, 1173, or 1373 K for 2 h and allowed to cool to room temperature. The XRD scans from the three experiments are shown in Figure 11. The presence of each phase was determined by the (111) tetragonal peak at $2\theta \sim 30°$ and the ($\bar{1}11$) and (111) monoclinic peaks at $2\theta \sim 28°$ and $2\theta \sim 31.5°$, respectively. During heating and the 2-h hold, only the tetragonal phase was seen. Upon cooling, the tetragonal phase transformed to the monoclinic phase. The temperature at which the first evidence of the monoclinic phase was seen was recorded as M_s, the tetragonal-to-monoclinic transformation start temperature. The transformation took place over the span of a few hundred degrees. For each maximum temperature, the crystallite size of the material was determined by X-ray line broadening of the (111) tetragonal peak. The relationships among maximum temperature, crystallite size, and M_s are shown in Figure 12. As we heated the sample to higher maximum temperatures, the crystallite size of the material increased, as did M_s.

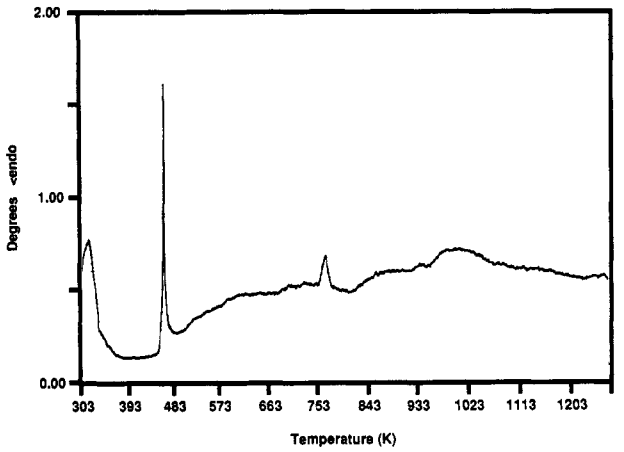

Figure 9. Differential thermal analysis scan of a ZrO_2 aerogel (gel no. 73) vacuum dried at 383 K for 3 h.

Cooling after heating to high temperatures caused the tetragonal phase to transform to the monoclinic phase. We also wanted to determine if prolonged heating at a lower temperature would cause the T → M transformation to occur. A tetragonal zirconia (Gel No. 82, previously heated at 773 K for 2 h in oxygen) was placed in a 773 K furnace with an air environment. Parts of the sample were removed after 24, 50, 100, 150, and 200 h, and then their structure and crystallite size were determined by XRD (see Figure 13). After heating at 773 K for a day or more, the initially tetragonal aerogel partially transformed to the monoclinic phase.

A similar in situ XRD experiment was performed to determine whether the transformation took place while holding at 773 K or upon cooling as was observed above. The sample (gel no. 82) was heated in the diffractometer to 773 K and held for 24 h. X-ray scans taken during this hold are shown in Figure 14a–c. The sample remained unchanged during the first seven hours (Figure 14a). During the next 14 h (Figure 14b), a small amount of the tetragonal phase converted to the monoclinic phase as seen by the emergence of the two monoclinic peaks. During the last 3 h (Figure 14c), there appeared to be no more growth in the monoclinic phase. However, it was uncertain whether the transformation actually stopped or if the three hour time span examined was too short to see any growth. Upon cooling to room temperature, there was a larger amount of transformation into the monoclinic phase (see Figure 14d). The crystallite size of the material and the tetragonal phase volume fraction during this experiment are shown in Figure 15.

Effect of Gel Time. To investigate more thoroughly the effect of gel time on zirconia aerogels, another series of zirconia gels was formed. At a water to zirconium ratio of 2.0, the acid amount was changed to affect gel time. When no acid was used, a precipitate was formed. This precipitate was simply filtered and washed, instead of extracted, before the standard heat treatment. Table II, series C summarizes the gels made in this series. As shown in Figure 16, the change in surface area and pore volume with gel time was qualitatively the same as the change in surface area with acid amount. This is expected since the acid amount controls the gel time. The precipitate had a much lower surface area and pore volume. The pore size distributions of these materials are shown in Figure 17. The 8- and 20-s gel times had narrow pore size distributions centered around 60–80 Å, while the precipitate and long gel time sample had broad distributions with maxima around 200–400 Å.

The gel time also affected the crystallite size of the material. All samples were tetragonal after calcination at 773 K for 2 h. The broadening of the (111) peak was used to determine crystallite size (see Figure 18). This crystallite size followed the reverse trend of the surface area. The low surface area precipitate had a large crystallite size. Aerogels prepared with intermediate gel time (8, 20, and 35 s) had large surface area and small crystallite size. Longer gel times increased the crystal size while decreasing the surface area. This crystallite size did not change significantly between the 773 and 973 K heat treatments (see Figure 19).

On the other hand, the crystal phase of the aerogels did change upon heating to 973 K, and this new phase composition was also a function of gel time. Figure 20 shows the tetragonal-to-monoclinic volume ratio vs gel time after this heat treatment. The precipitated sample completely transformed to the monoclinic phase. However, longer gel times retarded the transformation. Increasing gel time increased the volume fraction of the tetragonal phase. Any differences due to gel time (excluding the precipitate) were removed after heat treatment to 1173 K. All the samples were monoclinic and the crystallite sizes were nearly the same.

Discussion

Sol–Gel Parameters. Even though the actual sol–gel chemistry is complex, qualitatively it can be thought of in terms of the following two steps:

hydrolysis

$$M(OR)_n + xH_2O \rightarrow M(OR)_{n-x}(OH)_x + xROH \quad (1)$$

condensation

$$M\text{–}OH + HO\text{–}M \rightarrow M\text{–}O\text{–}M + H_2O \quad (2a)$$

$$M\text{–}OR + HO\text{–}M \rightarrow M\text{–}O\text{–}M + ROH \quad (2b)$$

During the hydrolysis step, a nucleophilic substitution occurs when the negative partial charge of the oxygen in water attacks the electropositive metal atom. A proton shift from the water to an –OR group creates an alcohol leaving group. The condensation step also consists of a nucleophilic substitution. The oxygen electrons of an M–OH group attack the metal atom of either an M–OH (eq 2a) or M–OR (eq 2b) group. Again, a proton shift creates a leaving group of either ROH or HOH. Thus, an M–O–M bridge is formed.

The rates of these two reactions determine the type of product formed. Generally, fast hydrolysis with slow condensation yields a polymeric gel.[9] Specifically, the hydrolysis of zirconium alkoxide is very fast. Zirconium is one of the most electropositive transition metals, giving it a favorable partial charge for the nucleophilic substitution reaction to occur. Experimentally, this fast hydrolysis was seen by the immediate precipitation of zirconia upon the addition of water to zirconium *n*-propoxide without the presence of nitric acid (gel no. A6, series C). The addition of nitric acid will only speed up the hydrolysis rate by protonating the –OR ligand, providing a better leaving group.

Even with the fast hydrolysis of zirconium alkoxide, a polymeric gel can be formed with the addition of acid.[25] Our data (Figure 2) show that the addition of acid not only prevented precipitation but also increased the gel time by decreasing the rate of condensation. Qualitatively,

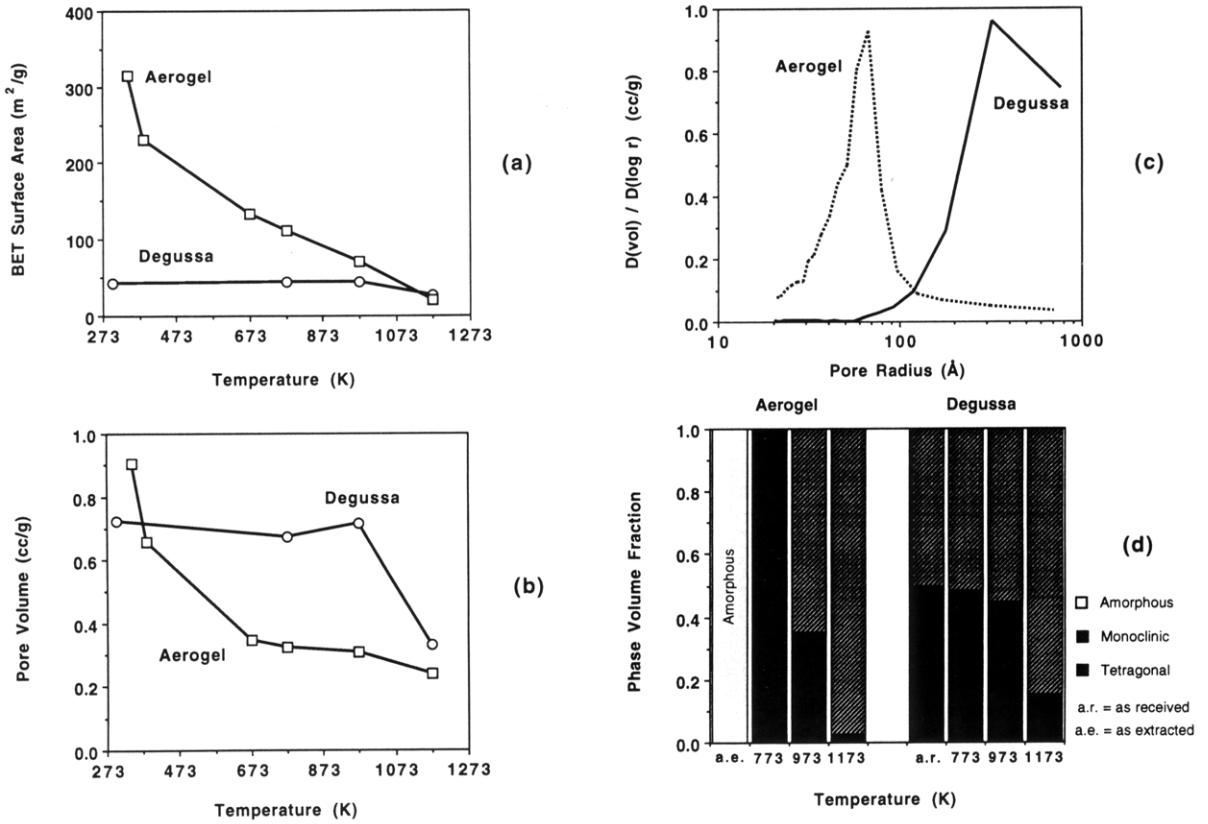

Figure 10. Comparison of ZrO_2 aerogel (gel no. 73) and Degussa ZrO_2 in terms of (a) surface area vs heat treatment, (b) pore volume vs heat treatment, (c) pore size distribution (for samples calcined at 773 K for 2 h; data points omitted for clarity), and (d) crystal structure as determined by X-ray diffraction vs heat treatment.

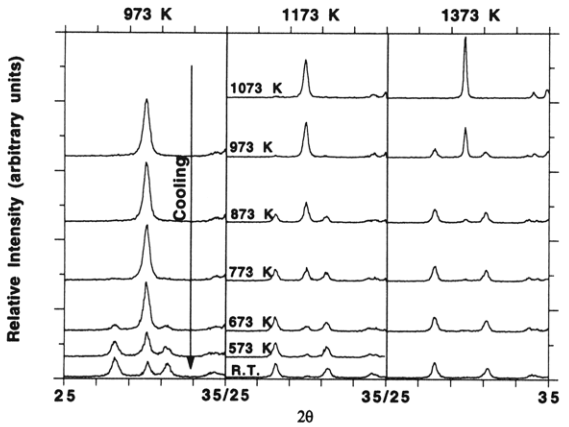

Figure 11. In situ X-ray diffraction patterns of zirconia aerogel (gel no. 75). Each panel represents a sample that was heated to the temperature indicated at the top, held at that temperature for 2 h and cooled.

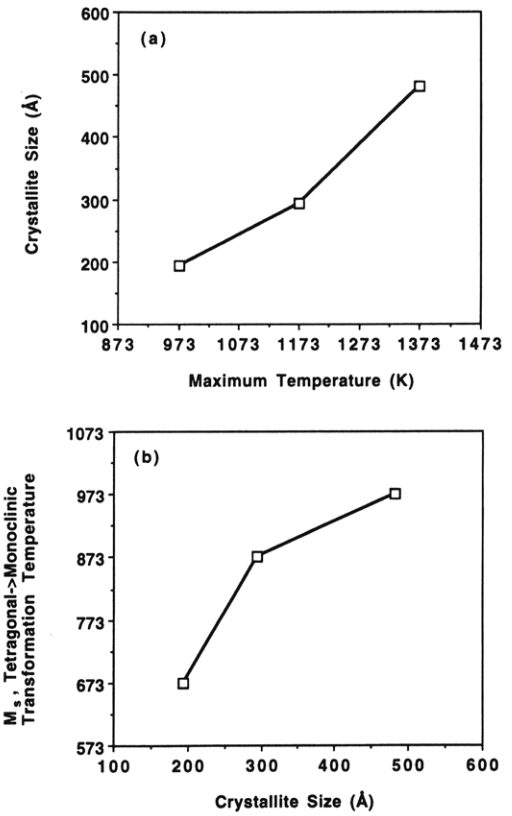

Figure 12. Summary of the in situ X-ray diffraction results in terms of (a) crystallite size vs maximum temperature and (b) M_s vs crystallite size.

the condensation rate is inversely proportional to gel time. With the addition of enough acid, condensation can be prevented entirely.[9] This can be explained by the protonation of the hydroxo ligands. The –OH ligands of the metal atom are protonated to form $M–OH_2^+$. The oxygen atom is no longer nucleophilic, decreasing the driving force for substitution. As more acid is added to the system, more hydroxo ligands are protonated and the condensation reaction slows, increasing the gel time. Livage *et al.*[9] stated that condensation is severely retarded as $[H^+]/[metal]$ approaches one. We found this same result. The gel time drastically increased approximately as $[HNO_3]/[Zr^{4+}]$ approached 1.0 (see Table II, column 4).

The amount of water used in the synthesis also affects the gel time. When the water ratio was decreased from 4.0 to 2.0 at a constant acid amount, the gel time increased (Figure 2). The decrease in water available for hydrolysis reduced the number of M–OH groups present. This decrease in concentration of M–OH groups slowed down the condensation reaction, increasing the gel time. We

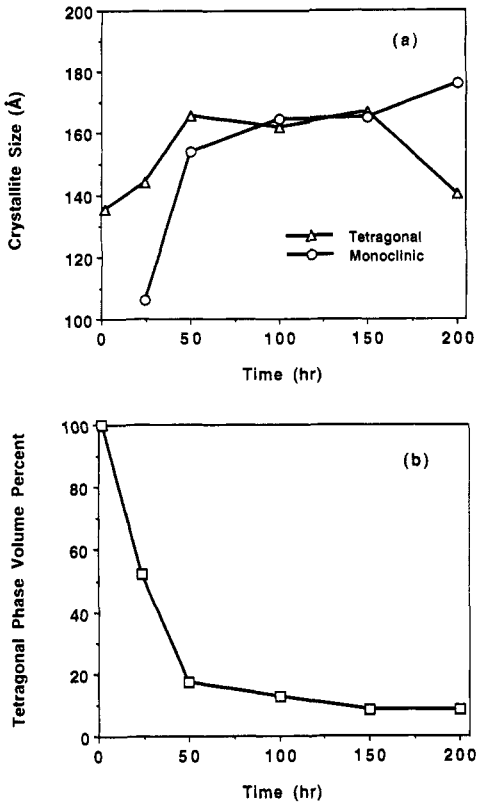

Figure 13. Effect of prolonged heating of a ZrO_2 aerogel (gel no. 82) at 773 K: (a) variation of crystallite size of tetragonal (△) and monoclinic (○) ZrO_2 with time, and (b) variation of tetragonal phase volume percent with time.

also observed, as did Yoldas,[25] that as more water was added to the system, more acid was needed to prevent precipitation. The increased amount of water caused an increased number of M–OH groups. Thus, more acid was required to protonate these extra M–OH groups in order to keep condensation slow and avoid precipitation.

We believe that the surface area variation with acid and water ratio, as shown in Figure 3, is actually a function of gel time. The effect of different gel times on the properties of zirconia is discussed in a later section.

Heat Treatment. A study of the effect of heat treatment on zirconia aerogels was performed on a sample prepared with a water ratio of 2.0 and an acid amount of 1.90 mL (Figures 4–9). Surface area and pore volume collapse did occur with heat treatment. However, our values of surface area and pore volume after calcination at 773 K compared very favorably with those in the literature (see Table I) for pure zirconia. Our aerogel synthesis does contain some batch-to-batch variations, even when all synthesis parameters are the same. However, with optimized sol–gel parameters, we consistently formed zirconia aerogels with a surface area of over 120 m^2/g after 773 K calcination. The highest observed surface area was 134 m^2/g. While the surface area was comparable to that of Duchet *et al.*,[31] the pore volume of our material was at least twice that of any other reported in the literature after this heat treatment. We also compared our aerogel to a commercial zirconia sample (Degussa, Figure 10). Our surface area was a factor of 3 higher after 773 K. While the Degussa zirconia had a larger pore volume, it consisted primarily of macropores (see Figure 10c). The aerogel was mesoporous (see Figure 5). Upon heat treatment at 773 K, most of the pores with radii of 100 Å or larger collapsed. Further heat treatment to higher temperatures caused the remaining, small pores to grow in size.

After extraction, the aerogel was X-ray amorphous. Upon heating to ca. 473 K, impurities such as residual organics and nitrate groups were released from the material. This event was highly exothermic as can be seen by the strong DTA peak at 473 K (Figure 9). With further heating, the material formed small tetragonal crystallites. The exact temperature at which crystallization began is uncertain. While X-ray diffraction of a material which had been heated at 673 K for 2 h showed no evidence of crystallinity, HRTEM showed that the aerogel did contain small tetragonal crystallites. DTA showed an exothermic peak around 773 K which corresponded to the crystallization of the material, but the temperature program of the DTA scan was a continuous ramp with no hold, unlike the calcination procedure. Although no exact temperature can be pointed to as the "crystallization temperature", we note that the crystallization into the tetragonal phase took place in the temperature range 673–773 K, depending on how the sample was heated. Further heat treatment converted the tetragonal phase to the monoclinic phase, either by prolonged heating at 773 K (Figure 13) or by heating to higher temperatures (Figures 6 and 7). By the aerogel preparation, we were able to stabilize zirconia into either a completely X-ray amorphous, or completely tetragonal, or completely monoclinic material, simply by changing its heat treatment. The commercially available zirconia to which we compared our sample was a mixture of the tetragonal and monoclinic phases, regardless of heat treatment, in the range of temperatures studied (Figure 10d).

Low-Temperature Tetragonal Phase and T→M Transformation. *Background.* As mentioned above, the existence of a low-temperature tetragonal phase seems to be in direct conflict with the phase diagram of bulk zirconia. However, many zirconia samples have been reported in the literature to be in the tetragonal phase at room temperature. This tetragonal phase is then converted to the monoclinic phase after heat treatment. Many explanations have been advanced for these observations. Garvie[42–44] first theorized that the tetragonal phase is stabilized by a crystallite size effect. While the monoclinic phase has a lower bulk free energy, the tetragonal phase has a lower surface free energy. For crystallites below a certain critical size, the surface energy term dominates the bulk energy term, stabilizing the tetragonal phase. Others proposed the formation of the tetragonal phase due to the short range structural similarities between the amorphous phase and the tetragonal phase.[45,46] Osendi *et al.*[47] stated that lattice defects created by the evolution of impurities during crystallization can nucleate the tetragonal phase. Srinivasan *et al.*[33] cited the pH and time of precipitation as controlling into which phase the zirconia crystallized.

Other explanations focus on the tetragonal-to-monoclinic transformation, or lack thereof, to explain the stabilized tetragonal phase. Domain boundaries have been shown experimentally to inhibit the transformation due to the strain that would be caused by the transformation of one particle surrounded by untransformed particles.[48]

(42) Garvie, R. C. *J. Phys. Chem.* **1965**, *69*, 1238.
(43) Garvie, R. C. *J. Phys. Chem.* **1978**, *82*, 218.
(44) Garvie, R. C.; Goss, M. F. *J. Mater. Sci.* **1986**, *21*, 1253.
(45) Livage, J.; Doi, K.; Mazieres, C. *J. Am. Ceram. Soc.* **1968**, *51*, 349.
(46) Tani, E.; Yoshimura, M.; Sōmiya, S. *J. Am. Ceram. Soc.* **1983**, *66*, 11.
(47) Osendi, M. I.; Moya, J. S.; Serna, C. J.; Soria, J. *J. Am. Ceram. Soc.* **1985**, *68*, 135.

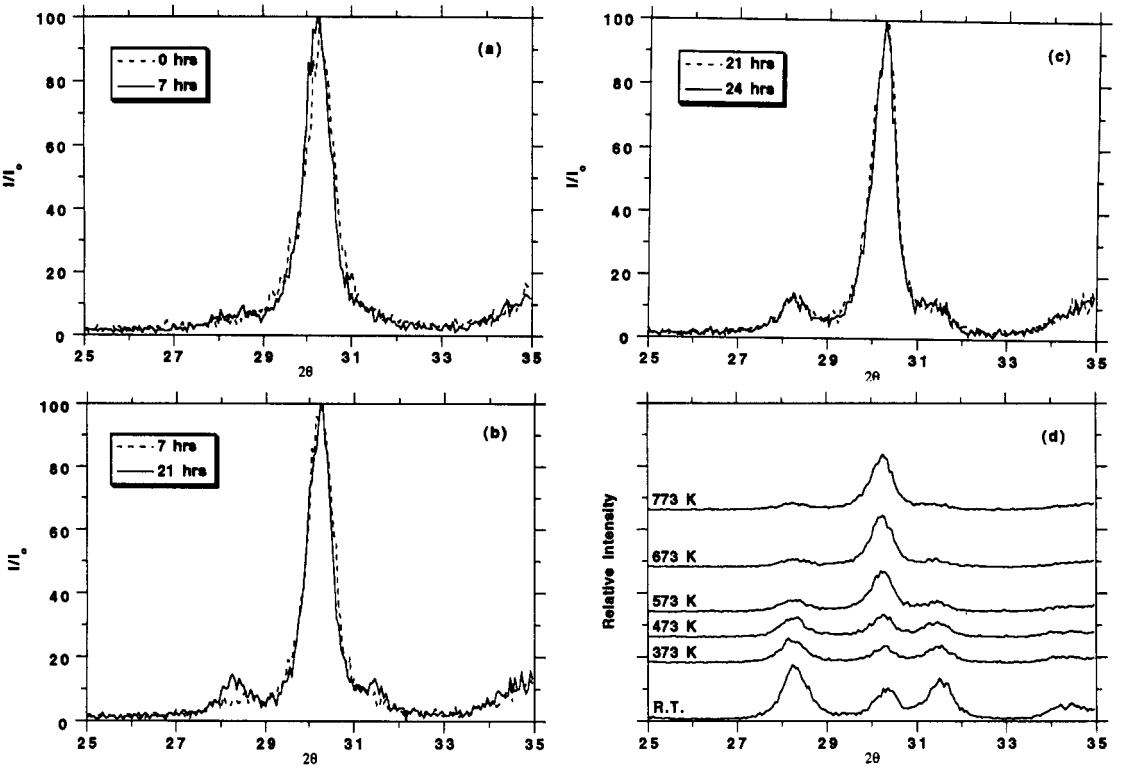

Figure 14. In situ X-ray diffraction patterns of a ZrO_2 aerogel (gel no. 82) heated at 773 K for (a) 0–7 h, (b) 7–21 h, (c) 21–24 h, and (d) subsequently cooled to room temperature.

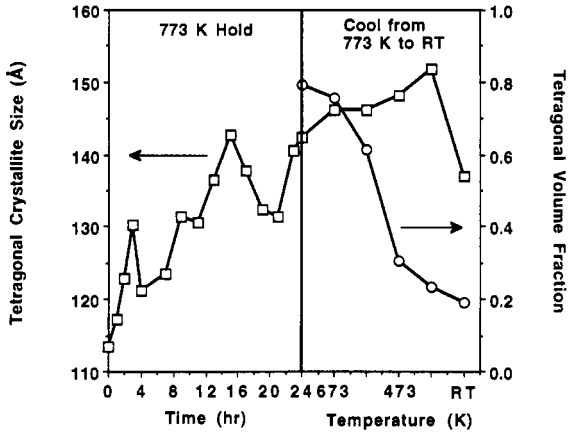

Figure 15. Summary of in situ XRD results for a ZrO_2 aerogel (gel no. 82) heated at 773 K for 24 h and then cooled. The left panel shows the tetragonal crystallite size (□) as a function of heating time at 773 K. The right panel shows the tetragonal crystallite size (□) and volume fraction (○) as a function of temperature upon cooling.

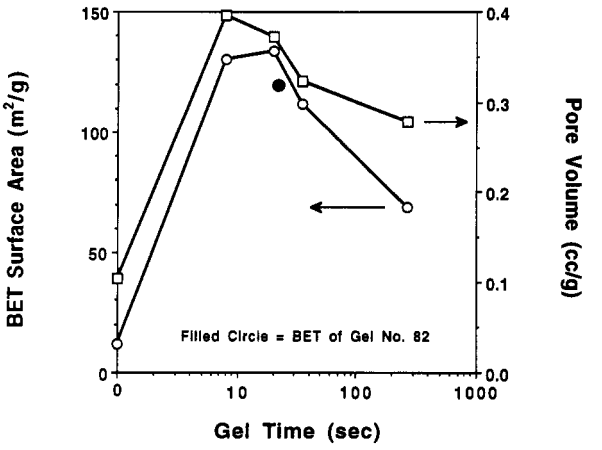

Figure 16. Effect of gel time on the surface area and pore volume of ZrO_2 aerogels (gel series C) after calcination at 773 K for 2 h.

Another theory states that a nucleation site must be present for the transformation to occur. A low-temperature tetragonal phase is stabilized due to the lack of nucleation sites, and the formation or growth of nuclei allows for the transformation. However, the theories on the nature and formation of nuclei are varied.[49-51] Andersson and Gupta[52] argued for the existence of pre-existing embryos. In a tetragonal zirconia sample, embryos of unknown origin exist and grow upon cooling below a temperature designated M_s. When an embryo reaches a critical size, it transforms the domain in which it is located. This theory can be used to explain a crystallite size effect. The probability of a crystallite containing an embryo at the critical size is proportional to the crystallite size. A material with large crystallites will thus show more T→M transformation upon cooling.

In Situ XRD Results. To more closely examine the tetragonal-to-monoclinic phase transformation, we examined an initially tetragonal zirconia sample by in situ X-ray diffraction. The first set of in situ experiments (Figure 11) followed the ex situ heat treatment conditions discussed above (heating at a set temperature for 2 h and then cooling). We found that the transformation from the tetragonal to monoclinic phase occurred when the sample was cooled. M_s, the temperature at which the first evidence of the monoclinic phase was seen, can be thought of as representing the boundary between the tetragonal and monoclinic phases on the phase diagram. However,

(48) Mitsuhashi, T.; Ichihara, M.; Tatsuke, U. *J. Am. Ceram. Soc.* **1974**, *57*, 97.
(49) Chen, I.-W.; Chiao, Y.-H. *Acta Metall.* **1985**, *33*, 1827.
(50) Heuer, A. H.; Claussen, N.; Kriven, W. M.; Rühle, M. *J. Am. Ceram. Soc.* **1982**, *65*, 642.
(51) Heuer, A. H.; Rühle, M. *Acta Metall.* **1985**, *33*, 2101.
(52) Andersson, C. A.; Gupta, T. K. In *Advances in Ceramics, Science and Advances in Zirconia*; Heuer, A. H., Hobbs, L. W., Eds.; American Ceramics Society: Columbus, OH, 1981; Vol. 3, pp 184–201.

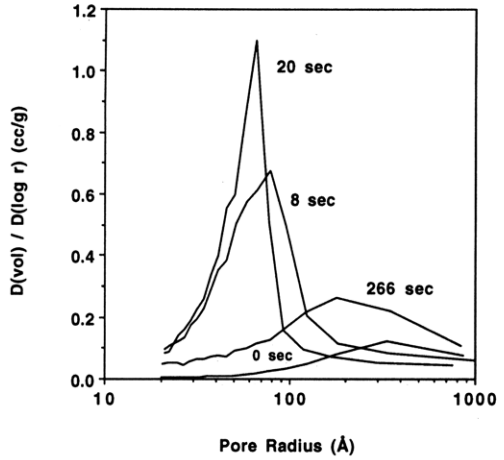

Figure 17. Effect of gel time on the pore size distribution of ZrO_2 aerogels (gel series C) after calcination at 773 K for 2 h. The data points are omitted for clarity.

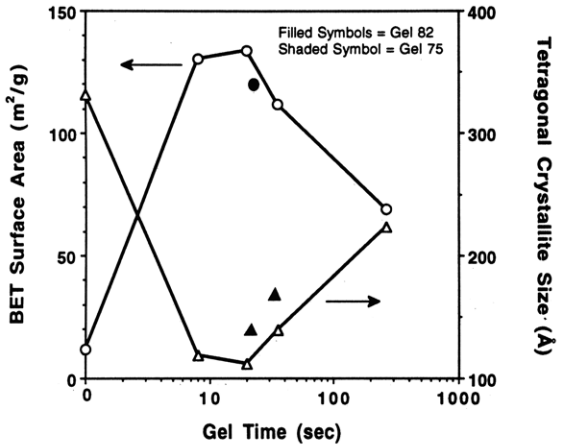

Figure 18. Effect of gel time on the surface area and tetragonal crystallite size of ZrO_2 aerogels (gel series C) after calcination at 773 K for 2 h.

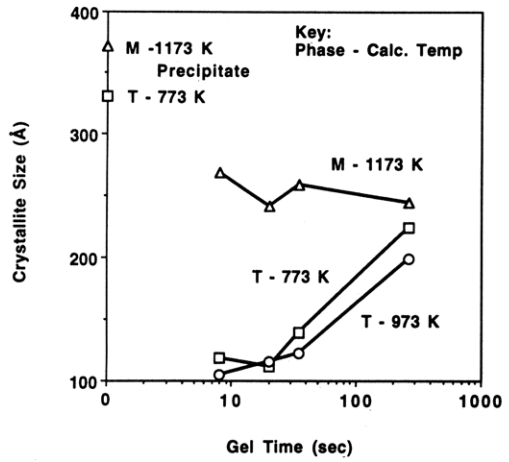

Figure 19. Effect of gel time on the crystallite sizes of tetragonal and monoclinic ZrO_2 (gel series C) after the samples had been calcined at the indicated temperature for 2 h.

this phase boundary does move depending on sample preparation and history; thus M_s is variable. The temperature of the sample must be below M_s for the monoclinic phase to exist. The transformation is athermal in nature and occurs over a range of temperatures.[40,41] The extent of transformation is a function of cooling below M_s. When the sample is cooled to a temperature slightly below M_s, only a portion of the tetragonal phase will transform to the monoclinic phase. Only a further decrease in temperature, providing an increase in the transformation

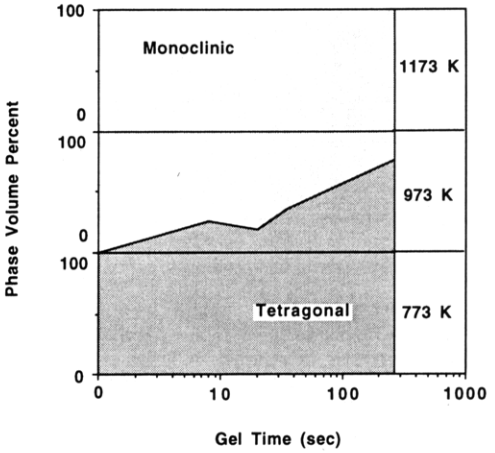

Figure 20. Effect of gel time on the structure of ZrO_2 aerogels (gel series C), as determined by X-ray diffraction, after the sample had been calcined at the indicated temperature for 2 h.

driving force, will continue the transformation until it is complete.

We examined the effect of the crystallite size on this transformation. In order to change the crystallite size of tetragonal ZrO_2, we performed this experiment at three different maximum temperatures (Figure 11). As we heated to higher temperatures, the crystallite size increased (Figure 12a). In addition, as the crystallite size increased, so did the M_s temperature (Figure 12b). M_s appears to be a function of crystallite size, with a larger crystallite size yielding a larger M_s.

The second in situ experiment was designed to mimic the prolonged heating at 773 K. Here, we saw that the transformation started during the hold at 773 K and continued during cooling (Figure 14). In addition, the ex situ experiment (Figure 13) shows that the longer the heating time at 773 K, the larger the amount of overall T → M conversion. These results can be interpreted in the following way. If at the end of the 773 K hold M_s is below room temperature, then upon cooling the temperature does not cross the boundary between the tetragonal and monoclinic phases which is represented by M_s. This is illustrated in Figure 21a. The zirconia sample remains in the tetragonal region of the phase diagram and is tetragonal at room temperature. If after the hold M_s is slightly above room temperature and the sample is cooled to room temperature, the transformation will begin but not finish (see Figure 21b). This sample will be a mixture of the two phases. Finally, if M_s is significantly larger than room temperature, the transformation will be complete upon cooling to room temperature, and the sample will be completely monoclinic (see Figure 21c). Given this explanation, we can determine the behavior of M_s during the 773 K hold of the aerogel. M_s was still below room temperature after 2 h (a tetragonal sample after cooling to room temperature) and went above room temperature by 24 h (a mixed tetragonal and monoclinic sample after cooling to room temperature). Since the monoclinic volume fraction increased with heating time, the transition region shown in Figure 21 moved up in temperature with heating time. This shows that M_s is a function of heating time. We will describe the mechanism behind this behavior of M_s below.

We note that the ex situ and in situ heating results at 773 K for 24 h differed in one quantitative aspect. The ex situ experiment yielded a zirconia that was 52% tetragonal upon cooling while the in situ experiment gave

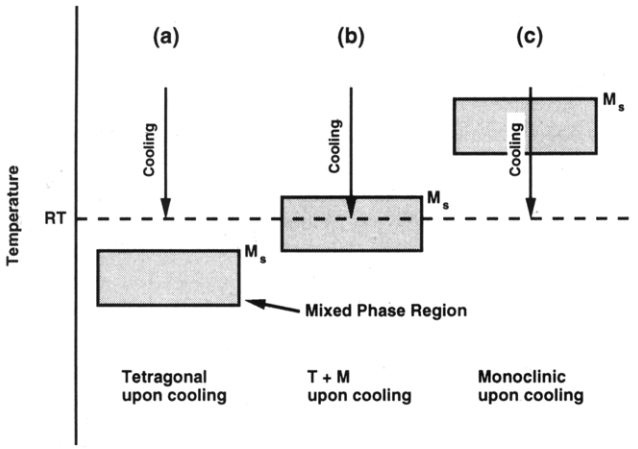

Figure 21. Schematic phase diagrams for zirconia samples with different M_s values. The shaded regions represent the temperature range over which the T → M transformation takes place. The tetragonal phase exists above the shaded region while the monoclinic phase exists below. (a) M_s is below room temperature so upon cooling the sample remains in the tetragonal phase. (b) M_s is slightly above room temperature so upon cooling the transformation begins and the material is a mixture of the tetragonal and monoclinic phases. (c) M_s is significantly above room temperature so upon cooling all of the material converts into the monoclinic phase.

a product with only 19% tetragonal phase. Differences in the experimental setup (for example, a benchtop furnace vs the in situ diffractometer furnace) may account for this variation as the transformation was very sensitive to the heat treatment conditions. This variation, however, did not affect our qualitative interpretation below.

Interpretation. A simple "critical crystallite size" as proposed by Garvie to account for a stabilized tetragonal phase is inadequate in explaining existing data. As pointed out by Srinivasan *et al.*,[53] tetragonal crystallites with sizes larger than monoclinic crystallites have been observed. Two examples of this can be found in our work. First, samples heated at 773 K for 24–150 h consisted of both the monoclinic and tetragonal phases (Figure 13). In these samples, the tetragonal phase had crystallites of either the same size or larger than the monoclinic phase. Second, the precipitated zirconia after calcination at 773 K was tetragonal with a crystallite size of 330 Å. These crystallites were larger than the monoclinic particles formed by heating an aerogel zirconia to 1173 K (see Figure 19). Since a tetragonal crystallite that is larger than a monoclinic crystallite can exist, the simple argument that crystallites below a certain size are tetragonal is not applicable to all situations.

The explanation put forth by Andersson and Gupta[52] also does not describe all of our observations. In their model, the preexisting embryos grow upon cooling. Thus, the T → M transformation should only be able to occur during cool down. However, we observed the transformation upon prolonged heating at 773 K (Figure 14a–c), which their model cannot explain.

We advance the following explanation for the crystallization behavior of zirconia. The aerogel is an initially amorphous material. As has been previously shown,[45,46] amorphous zirconia is structurally similar to the tetragonal phase. X-ray and neutron diffraction have shown that certain interatomic distances exist in the amorphous phase that are similar to distances found in the tetragonal phase. In other words, these two phases have similar short-range order. The energy barrier between the amorphous and tetragonal phases is less than that between the amorphous and monoclinic phases. Thus, upon heating, the amorphous material crystallizes into very small tetragonal crystallites, consistent with our HRTEM observations. These tetragonal crystallites grow as the material is heated.

Once in the tetragonal phase, the transformation to the monoclinic phase by way of homogeneous nucleation is very difficult due to a large activation energy barrier.[49] This barrier is lowered by providing a heterogeneous nucleation site, or embryo. An embryo is an intermediate structure between the tetragonal and monoclinic phase and is formed in a stress field in the crystallite. The origin of this stress field and formation of the embryo can be explained in two possible ways. In a classical heterogeneous nucleation model, a structural defect such as a dislocation loop or a Hertzian contact creates a stress field in the crystal for an embryo to grow.[49] The second approach is nonclassical and is called local soft mode (LSM) nucleation.[51] In this model, stresses at the crystallite interface create a stress field in the particle for an embryo to grow. This embryo does not have distinct boundaries but consists of a gradual transition from the parent crystal structure to the final martensitic embryo structure. For the embryo to form, the stress field must achieve a certain volume within the crystallite. The probability of achieving this critical volume is proportional to crystallite size, explaining a crystallite size effect. The data, as discussed to this point, do not allow us to distinguish between these two types of nucleation.

We believe the transformation occurs as follows. Embryos are formed in a range of embryo sizes (or efficiencies). This distribution of sizes is shown schematically in Figure 22a. Each embryo has a temperature below which it will convert its parent crystallite from the tetragonal to monoclinic phase. This temperature is designated M_s^{embryo}. This temperature is a function of embryo size, with larger embryo sizes (or efficiencies) having a larger M_s^{embryo}. In other words, a large embryo is better able to assist the transition. Since there is a range of embryo sizes, there is also a distribution of M_s^{embryo}. At a given temperature ($T_{current}$ in Figure 22a), all embryos with $M_s^{embryo} > T_{current}$ have converted their parent crystallite into the monoclinic phase (the shaded region in Figure 22a). The largest embryo, which also has the largest M_s^{embryo}, will transform its parent crystallite before any other. Since this occurrence of the first microscopic T → M transformation is also designated the temperature M_s, M_s for the sample must equal the largest M_s^{embryo}. The distribution of M_s^{embryo} within a sample accounts for the fact that the macroscopic T → M transformation is seen over a range of temperatures (the mixed phase region shown in Figure 21).

Upon heating, the embryos grow in size causing their M_s^{embryo} values to increase. If at anytime a tetragonal crystallite contains an embryo whose M_s^{embryo} is above the current temperature, the parent crystallite will transform to the monoclinic phase. Our data show this transformation in two ways. While heating at 773 K, the embryos grew to a size at which some values of M_s^{embryo} increased above 773 K (illustrated in Figure 22b), causing some tetragonal crystallites to transform while the sample was held at that temperature (Figure 14a–c). Also, cooling from elevated temperatures caused the transformation (Figures 11 and 14d). As a crystallite containing an embryo

(53) Srinivasan, R.; DeAngelis, R.; Davis, B. H. *J. Mater. Res.* **1986**, *1*, 583.

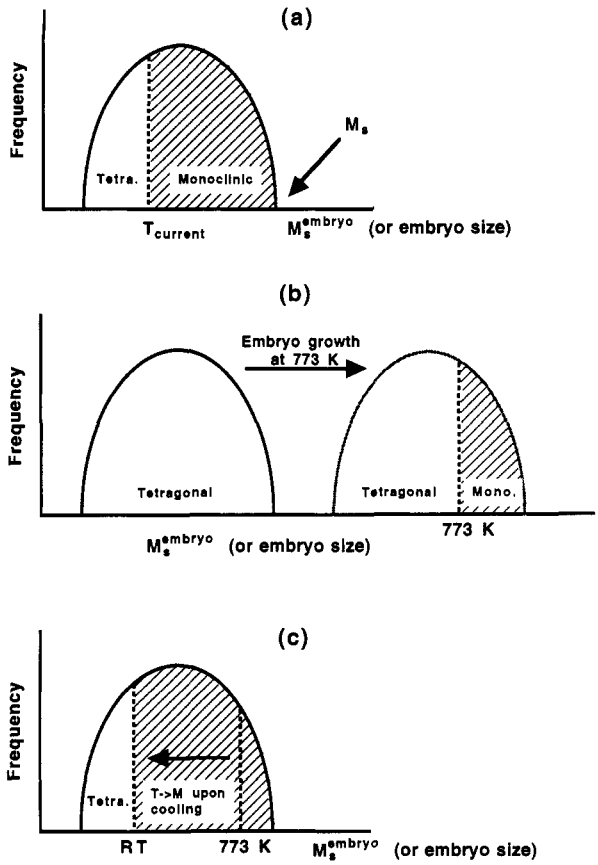

Figure 22. Illustration of M_s^{embryo} (or embryo size) distribution, embryo growth, and the T → M transformation. (a) The solid curve is a schematic of the M_s^{embryo} (or embryo size) distribution. The current temperature falls in the range of M_s^{embryo}. Crystallites containing an embryo with M_s^{embryo} above the current temperature have converted to the monoclinic phase. (b) This diagram shows the T → M conversion during prolonged heating. An initial distribution of embryo sizes (and hence M_s^{embryo}) are shown by the solid curve. All crystallites are tetragonal. Upon heating at 773 K, the embryos grow and the distribution curve shifts to larger sizes (to the location of the shaded curve). During this growth, some M_s^{embryo} values rise above the current temperature of 773 K causing those embryos to convert their parent tetragonal crystallites into the monoclinic phase. (c) This diagram shows the T → M conversion upon cooling after prolonged heating at 773 K. The sample temperature decreases to room temperature. All crystallites containing an embryo with M_s^{embryo} between 773 K and room temperature convert to the monoclinic phase.

cooled and the temperature decreased below the M_s^{embryo} of that embryo, the crystallite transformed to the monoclinic phase (illustrated in Figure 22c).

While this embryo size effect can explain all of our data, the direct evidence for a crystallite size effect must also be examined. The so-called crystallite size effect can be explained in one of the following ways. For the classical nucleation theory, we assume that there is a certain number of embryos per unit volume. The probability of a crystallite containing an embryo with a given M_s^{embryo} is proportional to the crystallite size. At a specific temperature T_0, for a crystallite to transform, it must contain an embryo with $M_s^{embryo} > T_0$. The probability of this occurrence increases with increasing crystallite size. Thus, the larger the average crystallite size of the material, the greater the probability that crystallites will have $M_s^{embryo} > T_0$, and the greater the amount of T → M conversion. A sample with a higher T → M conversion at a certain temperature has a higher sample M_s. For the nonclassical case, the formation of an embryo requires a critically sized stress field. Since this stress field is more easily formed in a larger crystallite, a larger crystallite has a higher probability for embryo growth. Samples with a large crystallite size have more embryo formation, more T → M conversion, and a larger M_s.

Experimentally, this relationship between crystallite size and transformation temperature was seen in the first set of in situ data (Figure 12). The samples with the larger crystallite sizes had a higher M_s. However, caution must be used in stating that M_s is solely a function of crystallite size. We propose that the embryo size also increases with temperature and that M_s is also a function of embryo size. From this set of data, it is difficult to separate the embryo size effect from the crystallite size effect. However, the prolonged heating in situ experiment (Figure 14) shows the importance of embryo size compared to crystallite size. During this experiment, there was only a small crystallite growth while there was a significant amount of T → M transformation. Thus, we believe that embryo size rather than crystallite size is the important factor governing the transformation, even though the latter has frequently been used as an apparent parameter in the literature.

This embryo growth interpretation can also explain the ex situ crystal structure determinations. Calcination of an amorphous zirconia at 773 K for 2 h caused the tetragonal phase to form in small crystallites with a distribution of small embryo sizes. M_s^{embryo} for all of the embryos was below room temperature (Figure 21a). So, the tetragonal phase was stable. Further calcination at 973 K for 2 h caused both the crystallite size and embryo size to grow. Some larger crystallites now contained a large embryo whose M_s^{embryo} was above room temperature. So, during cooling from 973 K to room temperature, such crystallites did transform (Figure 21b). Consequently, there was a mix of the tetragonal and monoclinic phase. Heat treatment at 1173 K for 2 h caused the embryos and crystallites to become sufficiently large such that every crystallite contained an embryo with M_s^{embryo} greater than room temperature (Figure 21c). Subsequent cooling caused all of the material to transform to the monoclinic phase. When a tetragonal material was held at 773 K for a period of time, the embryos grew while the crystallite size increased only slightly. With increased heating time at 773 K, the M_s^{embryo} distribution moved with time to higher temperatures allowing for a greater degree of T → M conversion (Figure 13).

Importance of Gel Time. Many of the above effects on the physical characteristics and crystal structure of the zirconia aerogel can be related to the gel time of the alcogel from which it was formed. First, the surface area and pore structure of the aerogels varied with gel time (Figure 16). When we used no acid, we formed a precipitate. The lack of acid allowed the condensation reaction to proceed very quickly. Individual particles grew rapidly with very little chance for bridging between particles. Hence, the calcined product had very little surface area and pore volume. However, with the use of acid, the condensation was slowed down so that more bridging could occur between small, growing particles. The resulting gel network had a large surface area and porosity. As the gel time lengthened further, the condensation reaction was slowed down so much that large particles formed with little bridging between them upon heating. This network contained large particles with less open space, and hence the surface area and pore volume decreased. Gels with the small bridged particles formed mesopores, while the precipitated and long gel time materials with continuous

large particles formed macropores (see Figure 17).

We could separate gel times into three categories: short (zero or precipitate), intermediate (5–45 s), and long (above 1 min). We qualitatively saw a difference between these categories. Gels within each time period often had very similar results and could not be further categorized by smaller gel time intervals due to batch to batch variation. In other words, the physical characteristics were not noticeably different between 10- and 20-s gels, but definitely so between 20-s and 2-min ones.

After calcination at 773 K for 2 h, all samples were in the tetragonal phase and the tetragonal crystallite size was a function of gel time. In fact, it appeared to be a function of gel time in the opposite way that the surface area was a function of gel time (Figure 18). At gel times when the surface area was large, the crystallite size was small, and vice versa. We provide the following explanation. At intermediate gel times, the network was open and porous, impeding crystallite growth. On the other hand, the large particles found in the precipitate and long gel time sample allowed for easy crystal growth. The effect of gel time, which can explain the surface area variations, can be used in the same way to account for the varying crystallite size.

The variation of crystallite size with gel time was the same after both 773 and 973 K heat treatments (Figure 19). Except for the precipitate, increasing gel times gave a larger crystallite size. However, the structure of the materials changed after the 973 K heat treatment (Figure 20). The precipitate was completely monoclinic, and with increasing gel time, the fraction of tetragonal phase remaining also increased.

This is a very important result. In the above in situ XRD experiments, we changed the crystallite size of the material by heating to different temperatures. We saw a relationship between crystallite size and the T → M transformation. Increased crystallite size appeared to cause a greater degree of T → M transformation upon cooling to room temperature. By changing the gel time, we now have an alternate method of controlling the crystallite size. With this method, we find results opposite to that above. With increasing crystallite size as caused by longer gel time, we actually saw less of a transformation to the monoclinic phase. This reinforces our earlier notion that crystallite size alone cannot account for the tetragonal-to-monoclinic phase transformation data.

Again, the embryo model can explain this paradox. We can now assert that the classical nucleation model best describes this data. In the nonclassical LSM model, the crystallite size of the material is directly tied to the ability of the material to transform. Large crystallite materials can more easily form embryos and hence will transform to a greater degree. The data showed the exact opposite trend. Hence, this model does not apply to this system. The classical model does apply to our system with one small modification. The crystallite size effect in the classical theory hinges on the fact that the number of embryos per volume is a constant. However, by changing the gel time, we in essence have a novel way to change this density of embryos. The precipitated sample formed very quickly causing many imperfections to exist in the network. This large number of defects served as nucleation sites for embryos. As the gel time increased, the zirconia structure formed at a slower pace and fewer defects were incorporated into the structure. This caused fewer embryos to form. Finally, a long gel time gave the network a chance to build itself in such a way that even fewer defects existed. As the number of defects, and hence embryos, decreased with gel time, the fraction of embryos that were of a critical size to transform after 973 K also decreased. Thus, as gel time increased, the amount of T → M transformation decreased as shown by the data.

Finally, after calcination at 1173 K, the effect of gel time had been annealed out. All samples were completely monoclinic and had virtually the same crystallite size, except for the precipitate which started with a much larger crystallite size.

Conclusions

We synthesized a zirconia aerogel using the sol–gel method and supercritical drying. By optimizing the sol–gel parameters in the synthesis, we prepared an aerogel with a high surface area (ca. 130 m^2/g after 773 K for 2 h) and moderate thermal stability with heating. With this preparation, we were also able to stabilize both an amorphous and tetragonal phase at room temperature. No doping or stabilizers were required to obtain either of these results. Since many commercial zirconia samples are either a mixture of phases or are doped to obtain a single phase, our aerogel will allow for the use of a single phase, high surface area, pure zirconia in catalytic applications.

The formation of a low-temperature tetragonal phase zirconia allowed us to examine the tetragonal-to-monoclinic transformation. We believe it is controlled by an embryo formation and growth phenomenon. Defects formed during the aerogel synthesis provided nucleation sites for embryo formation. These embryos grew with heating and their size determined at what temperature the T → M transformation occurred. When the sample temperature fell below this transformation temperature, the embryo caused its parent crystallite to transform. This model, developed to explain new in situ and ex situ heat treatment results in this study, resolves some apparent discrepancies in the literature on the structural transformation of zirconia.

We showed that gel time, which can be controlled by varying the acid content in the synthesis, is a crucial parameter in affecting the physical characteristics of the zirconia aerogel. At a macroscopic level, gel time influenced the gel network that was formed and, in turn, the morphology and crystallite size of a particular structure upon heat treatment. At a microscopic level, gel time changed the "quality" of the material in terms of defect density. These results are significant in showing that there is a low-temperature method for changing crystallite size as well as embryo density and that crystallite size alone is an insufficient parameter in fully explaining the tetragonal-to-monoclinic transformation.

Acknowledgment. This work was partially supported by the National Science Foundation (CTS-9200665). D.A.W. thanks the Texaco Foundation for the support of a graduate fellowship. We also acknowledge W. S. Hammack, J. G. Wolf, and A. Garg for their help in Raman, in situ XRD, and HRTEM measurements, respectively, and Degussa Corporation for supplying us with the ZrO_2 sample.